

Autofrettage process analysis of a compound cylinder based on the elastic-perfectly plastic and strain hardening stress-strain curve[†]

Eun-Yup Lee¹, Young-Shin Lee^{1,*}, Qui-Ming Yang¹, Jae-Hoon Kim¹, Ki-Up Cha²
and Suk-Kyun Hong²

¹*BK21 Mechatronics Group, Department of Mechanical Design Engineering, Chungnam National University, Daejeon, 305-764, Korea*

²*Agency for Defense Development, 111 Sunam-dong Yuseong-gu, Daejeon, 305-152, Korea*

(Manuscript Received November 14, 2008; Revised June 4, 2009; Accepted August 19, 2009)

Abstract

The autofrettage process enhances the carrying capacity and fatigue lifetime of pressure vessels by increasing their residual stress. A compound cylinder was introduced in order to increase residual stress. An autofrettaged compound cylinder can resist a higher pressure than a single cylinder having the same dimension. This residual stress can be measured through experimental or calculation processes. In this study, residual stress analysis of an autofrettaged compound cylinder was conducted. The elastic-perfectly plastic and strain hardening models were investigated. The residual stress distribution of the autofrettaged compound cylinder with shrink fit tolerance was predicted. Shrink fit is a very efficient way to extend compressive residual stress. The compressive residual stress of the strain-hardening model is smaller than that of the elastic-perfectly plastic model because of the Bauschinger effect. The compressive residual stress of the strain hardening model decreased by up to 80% overstrain level.

Keywords: Autofrettage process; Compound cylinder; Elastic-perfectly plastic model; Strain hardening model

1. Introduction

The autofrettage process is used to enhance the carrying capacity and fatigue lifetime of pressure vessels by introducing compressive residual stress into them. A multi-layered cylinder was proposed by Kapp et al. [1] in order to introduce compressive residual stress. A multi-layered cylinder manufactured through a shrink fit process can withstand higher pressure than a single cylinder having the same dimensions.

Milligan et al. [2] showed the influence of the Bauschinger effect, which reduces yield strength as a result of prior tensile plastic overload, in high strength steel. The compressive residual stress of an autofrettaged cylinder reduces the nearby inner radius be-

cause of the Bauschinger effect. The Bauschinger effect factor is a function of plastic strain, and this dependency was formulated by Kendall [3].

The autofrettaged model using the elastic-perfectly plastic model was proposed by Hill [4]. It is limited in accuracy because of the Bauschinger effect and strain hardening [5]. However, the strain-hardening model considers the Bauschinger effect and strain-hardening by using close curve-fitting ability. Therefore, it can give more accurate results than the elastic-perfectly plastic model. Huang [6, 7] studied the autofrettaged single cylinder model using the tensile-compressive curve of the material.

Park et al. [8-10] examined the residual stress of a compound cylinder using the elastic-perfectly plastic model after the autofrettage process. The residual stress of a compound cylinder at the inner radius was increased with the overstrain level. Moreover, the compressive residual stress of a compound cylinder at

[†] This paper was recommended for publication in revised form by Associate Editor Jooho Choi

*Corresponding author. Tel.: +82 42 821 6644, Fax.: +82 42 821 8906

E-mail address: leeys@cnu.ac.kr

© KSME & Springer 2009

the inner radius was increased after the inner radius was machined. Lee and coworkers [11] investigated the fatigue life of the autofrettaged compound cylinder.

In this study, residual stress analysis of the autofrettaged compound cylinder was conducted. The elastic-perfectly plastic and strain hardening models were investigated. The residual stress distribution of the autofrettaged compound cylinder with shrink fit tolerance was predicted.

2 Residual stress of a compound cylinder

2.1 Material and stress-strain curve

The single cylinder was made up of AISI 4340, a high-strength steel. The residual stresses of the single cylinder were calculated through two ways, namely, elastic-perfectly plastic analysis and strain hardening analysis. The difference between these two lies in the simplification of the stress-strain curve that is used to calculate residual stress.

The actual stress-strain curve [11] of AISI 4340 is shown in Fig. 1. The general stress-strain curve shown in Fig. 2 is divided into four zones: O-A, A-B, B-D, and D-E. The O-A and B-D zones are linear elastic zones, while the A-B and D-E zones are the strain hardening zone. Table 1 shows the mechanical properties of AISI 4340.

2.2 Elastic-perfectly plastic analysis

The elastic-perfectly plastic model uses linearly simplified stress-strain curve. The yield strength and Young’s modulus of AISI 4340 were only needed to calculate residual stress. The Bauschinger effect and strain hardening are not reflected in residual stress analysis. Therefore, zones B-D and D-E, as shown in Fig. 3, are flat and are represented by straight lines and yield strength (σ_{y+}) during the unloading phase (B-C-E), with the latter being equal to the yield strength (σ_{y-}) during the loading phase (O-A-B).

Table 1. Mechanical properties of AISI 4340 [11].

Young’s modulus, E (GPa)	205
Tensile strength, ρ_t (MPa)	1272
Elongation, EL (%)	19
Yield strength, σ_y (MPa)	1180
Poisson’s ratio, ν	0.29

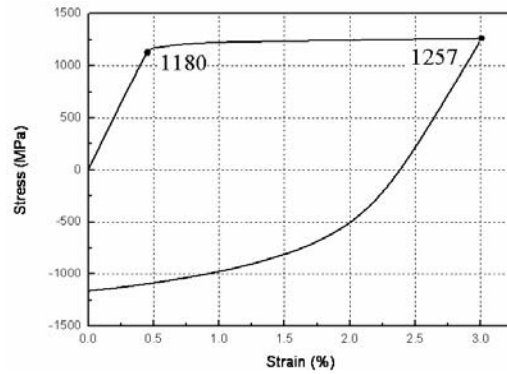


Fig. 1. Stress-strain curve of AISI 4340 [11].

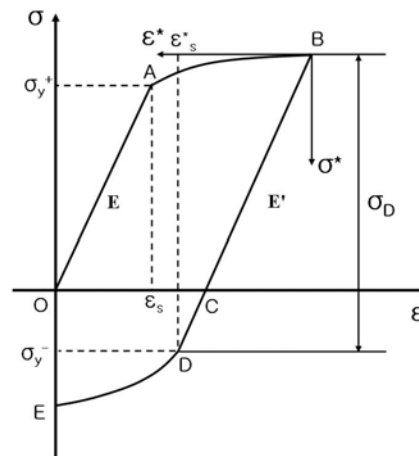


Fig. 2. General tensile-compressive stress stress-strain curve of strain hardening material [11].

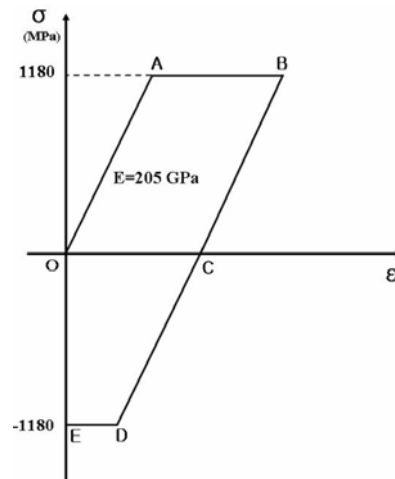


Fig. 3. Simplified stress-strain curve of the elastic-perfectly plastic model.

Table 2. Calculation parameters of AISI 4340 [11].

σ_y	E (GPa)	A ₁ (MPa)	A ₂ (MPa)	B ₁	σ_D (MPa)	E' (GPa)	A ₃ (MPa)	A ₄ (MPa)	B ₂
1180	205	1165	3384	1.0	1742	178	0.49	3826	0.44

Material behaves in elastic-perfectly plastic in residual stress analysis, elastic unloading was supposed for calculation. The residual stress of a compound cylinder subjected to autofrettage pressure can be expressed through the Lamé equation. The cross-section of autofrettaged single cylinder using the elastic-perfectly plastic model is shown in Fig. 4.

The residual stress of an autofrettaged single cylinder is derived using the following equations [12]:

- Residual stress in the plastic zone ($r_i \leq r \leq r_c$)

$$\sigma_r^A = \sigma_y \left\{ \frac{r_i}{r_o - r_i} \left(1 - \frac{r_o^2}{r^2} \right) \left[\ln \frac{r_i}{r_c} - \frac{r_o - r_c}{2r_o^2} \right] + \left[\ln \frac{r}{r_c} - \frac{r_o^2 - r_c^2}{2r_o^2} \right] \right\} \quad r_i \leq r \leq r_c \quad (1)$$

$$\sigma_\theta^A = \sigma_y \left\{ \frac{r_i}{r_o - r_i} \left(1 + \frac{r_o^2}{r^2} \right) \left[\ln \frac{r_i}{r_c} - \frac{r_o - r_c}{2r_o^2} \right] + \left[\ln \frac{r}{r_c} + \frac{r_o^2 - r_c^2}{2r_o^2} \right] \right\} \quad r_i \leq r \leq r_c \quad (2)$$

- Residual stress in the elastic zone ($r_c \leq r \leq r_o$)

$$\sigma_r^A = \sigma_y \left(1 - \frac{r_o^2}{r^2} \right) \left[\frac{r_c^2}{2r_o^2} + \frac{r_i}{r_o - r_i} \left(\ln \frac{r_i}{r_c} - \frac{r_o^2 - r_c^2}{2r_o^2} \right) \right] \quad r_c \leq r \leq r_o \quad (3)$$

$$\sigma_\theta^A = \sigma_y \left(1 + \frac{r_o^2}{r^2} \right) \left[\frac{r_c^2}{2r_o^2} + \frac{r_i}{r_o - r_i} \left(\ln \frac{r_i}{r_c} - \frac{r_o^2 - r_c^2}{2r_o^2} \right) \right] \quad r_c \leq r \leq r_o \quad (4)$$

2.3 Strain hardening analysis [11]

The simplified stress-strain curve of the strain hardening model as shown in Fig. 5 is similar to the actual stress-strain curve. Therefore, the Bauschinger effect and strain hardening can be reflected in residual stress analysis using the strain hardening model. The cross-section of an autofrettaged single cylinder of the strain hardening model is shown in Fig. 6. Here a , c , ρ_L , ρ_U are the inner radius, outer radius, loading zone radius, and unloading zone radius, respectively.

Many parameters that are needed for calculating residual stress are obtained through curve fitting. Table 2 shows the parameters of AISI 4340 that are used for calculation. Residual stress was calculated by using these parameters.

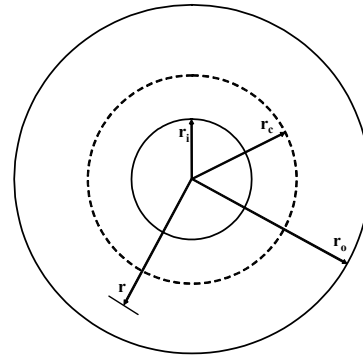


Fig. 4. Cross-section of an autofrettaged single cylinder using the elastic-perfectly plastic model.

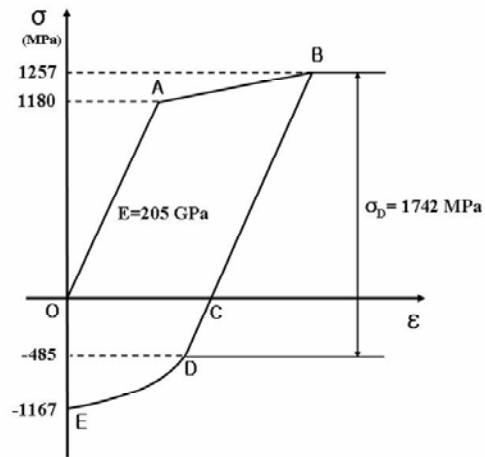


Fig. 5. Simplified stress-strain curve of the strain hardening model.

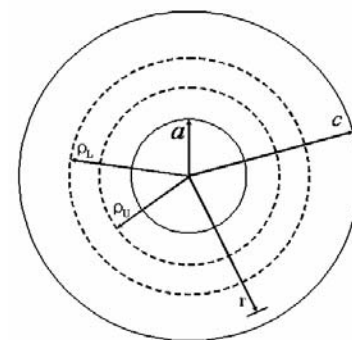


Fig. 6. Cross-section of an autofrettaged single cylinder using the strain hardening model.

Table 3. Calculation parameters of 30CrNiMo8 [7].

σ_y	E (GPa)	A_1 (MPa)	A_2 (MPa)	B_1	σ_D (MPa)	E' (GPa)	A_3 (MPa)	A_4 (MPa)	B_2
960.7	207	948.2	9157	1.0	1420	201	-5.0	10850	0.47

2.3.1 Loading stress analysis (σ^L)

Loading stress analysis is based on the Cartesian coordinate system (ε -O- σ) in Fig. 2. In the loading phase, the radius of the elasto-plastic zone is expressed as ρ_L in the loading stress zone. ρ_L depends on autofrettage pressure p_a . The formulation for calculating loading stress is expressed below. The calculation parameters in Table 2 are used in Eq. (5, 6).

(1) Plastic zone ($a \leq r \leq \rho_L$)

$$\sigma_r^{L1} = \frac{2}{\sqrt{3}} A_1 \ln\left(\frac{r}{a}\right) + \frac{\sigma_y - A_1}{\sqrt{3} B_1} \rho_L^{2B_1} \left(\frac{1}{a^{2B_1}} - \frac{1}{r^{2B_1}} \right) - p_a \quad (5)$$

$$\sigma_\theta^{L1} = \frac{2}{\sqrt{3}} A_1 \left[\ln\left(\frac{r}{a}\right) + 1 \right] + \frac{\sigma_y - A_1}{\sqrt{3} B_1} \rho_L^{2B_1} \left[\frac{1}{a^{2B_1}} + (2B_1 - 1) \frac{1}{r^{2B_1}} \right] - p_a \quad (6)$$

(2) Elastic zone ($\rho_L \leq r \leq c$)

$$\sigma_r^{L2} = \frac{\sigma_y}{\sqrt{3}} \rho_L^2 \left(\frac{1}{c^2} - \frac{1}{r^2} \right) \quad (7)$$

$$\sigma_\theta^{L2} = \frac{\sigma_y}{\sqrt{3}} \rho_L^2 \left(\frac{1}{c^2} + \frac{1}{r^2} \right) \quad (8)$$

2.3.2 Unloading stress analysis (σ^U)

Unloading stress analysis is based on the Cartesian coordinate system (ε^* -O- σ^*) in Fig. 2. In the unloading phase, the radius of the elasto-plastic zone is expressed as ρ_U in the unloading stress zone. The procedure of unloading stress analysis is the same as that of loading stress analysis. The formulation for calculating loading stress is expressed below.

(1) Plastic zone ($a \leq r \leq \rho_U$)

$$\sigma_r^{U1} = \frac{2}{\sqrt{3}} A_3 \ln\left(\frac{r}{a}\right) + \frac{\sigma_D - A_3}{\sqrt{3} B_2} \rho_U^{2B_2} \left(\frac{1}{a^{2B_2}} - \frac{1}{r^{2B_2}} \right) - p_a \quad (9)$$

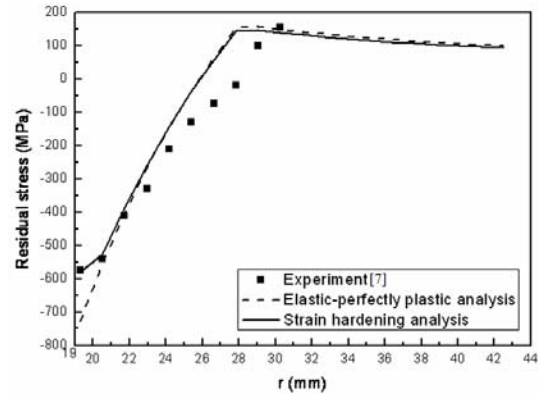


Fig. 7. Residual stress distribution of an autofrettaged single cylinder with 35.7% overstrain level.

$$\sigma_\theta^{U1} = \frac{2}{\sqrt{3}} A_3 \left[\ln\left(\frac{r}{a}\right) + 1 \right] + \frac{\sigma_D - A_3}{\sqrt{3} B_2} \rho_U^{2B_2} \left[\frac{1}{a^{2B_2}} + (2B_2 - 1) \frac{1}{r^{2B_2}} \right] - p_a \quad (10)$$

(2) Elastic zone ($\rho_U \leq r \leq c$)

$$\sigma_r^{U2} = \frac{\sigma_D}{\sqrt{3}} \rho_U^2 \left(\frac{1}{c^2} - \frac{1}{r^2} \right) \quad (11)$$

$$\sigma_\theta^{U2} = \frac{\sigma_D}{\sqrt{3}} \rho_U^2 \left(\frac{1}{c^2} + \frac{1}{r^2} \right) \quad (12)$$

2.4 Residual stress of a single cylinder using 30CrNiMo8 [7]

Huang [7] conducted an autofrettage experiment using 30CrNiMo8. A single cylinder was autofrettaged with 35.7% overstrain level. The autofrettage pressure was 740 MPa. The calculations were based on the following geometrical properties: $a = 19.3$ mm; $c = 43.7$ mm; $\rho_U = 28$ mm; and $\rho_L = 20.6$ mm. Table 3 shows the parameters of 30CrNiMo8 that were used for calculation. Residual stress was calculated by using these parameters.

Fig. 7 shows the tangential residual stress along the wall thickness of an autofrettaged single cylinder. This single cylinder was autofrettaged with 35.7% overstrain level. The maximum compressive residual

stress of the strain-hardening model shows consistency in the experiment. The compressive residual stresses at the inner radius and the tensile residual stresses at the outer radius decreased with the over-strain level.

2.5 Residual stress of a compound cylinder using AISI 4340

A compound cylinder as shown in Fig. 8 has been proposed in order to achieve very long fatigue lifetimes. This compound cylinder was manufactured through a shrink fit process. The residual stress distribution of a compound cylinder can change because of shrink fit. Therefore, the shrink fit stress needs to be reflected in residual stress. The calculations were based on the following geometrical properties: $a = 78$ mm; $b = 117$ mm; $c = 156$ mm; and $\delta = 0.1$ mm.

2.5.1 Shrink fit stress analysis

The compound cylinder was made through a shrink fit process. The inner radius of the outer cylinder may be made smaller than the outer radius of the inner cylinder. The cylinders are assembled after the outer cylinder is heated and the inner cylinder is cooled down. The contact pressure (p) between the cylinders can be calculated through Eq. (13).

$$p = \frac{\delta}{b} \cdot 1 / \left\{ \frac{1}{E_1} \left(\frac{a^2 + b^2}{b^2 - a^2} - \nu \right) + \frac{1}{E_2} \left(\frac{b^2 + c^2}{c^2 - b^2} - \nu \right) \right\} \quad (13)$$

In the inner cylinder, the contact pressure acts as an external pressure. However, the contact pressure is an internal pressure in the outer cylinder. The stress distribution of cylinders as a result of shrink fit [13] can be calculated through Eqs. (14-17).

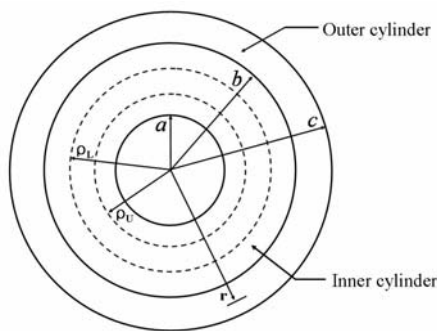


Fig. 8. Cross-section of an autofrettaged compound cylinder using the strain hardening model.

(1) Inner cylinder

$$\sigma_r^{s1} = -\frac{\delta}{b} \cdot 1 / \left\{ \frac{1}{E_1} \left(\frac{a^2 + b^2}{b^2 - a^2} - \nu_1 \right) + \frac{1}{E_2} \left(\frac{b^2 + c^2}{c^2 - b^2} + \nu_2 \right) \right\} \cdot \frac{b^2}{b^2 - a^2} \left(1 - \frac{a^2}{r^2} \right) \quad (14)$$

$$\sigma_\theta^{s1} = -\frac{\delta}{b} \cdot 1 / \left\{ \frac{1}{E_1} \left(\frac{a^2 + b^2}{b^2 - a^2} - \nu_1 \right) + \frac{1}{E_2} \left(\frac{b^2 + c^2}{c^2 - b^2} + \nu_2 \right) \right\} \cdot \frac{b^2}{b^2 - a^2} \left(1 + \frac{a^2}{r^2} \right) \quad (15)$$

(2) Outer cylinder

$$\sigma_r^{s2} = \frac{\delta}{b} \cdot 1 / \left\{ \frac{1}{E_1} \left(\frac{a^2 + b^2}{b^2 - a^2} - \nu_1 \right) + \frac{1}{E_2} \left(\frac{b^2 + c^2}{c^2 - b^2} + \nu_2 \right) \right\} \cdot \frac{b^2}{c^2 - b^2} \left(1 - \frac{c^2}{r^2} \right) \quad (16)$$

$$\sigma_\theta^{s2} = \frac{\delta}{b} \cdot 1 / \left\{ \frac{1}{E_1} \left(\frac{a^2 + b^2}{b^2 - a^2} - \nu_1 \right) + \frac{1}{E_2} \left(\frac{b^2 + c^2}{c^2 - b^2} + \nu_2 \right) \right\} \cdot \frac{b^2}{c^2 - b^2} \left(1 + \frac{c^2}{r^2} \right) \quad (17)$$

2.5.2 Residual stress analysis

Residual stress is calculated by using loading stress, unloading stress, and shrink fit stress, $\sigma^A = \sigma^L - \sigma^U + \sigma^S$.

When the plastic zone is in the inner cylinder ($a < \rho_L < b$), residual stress is expressed by Eqs. (18-21).

(1) Residual stress of the unloading stress zone ($a < r < \rho_U$)

$$\sigma_r^A = \sigma_r^{L1} - \sigma_r^{U1} + \sigma_r^{S1}, \quad \sigma_\theta^A = \sigma_\theta^{L1} - \sigma_\theta^{U1} + \sigma_\theta^{S1} \quad (18)$$

(2) Residual stress of the loading stress zone ($\rho_U < r < \rho_L$)

$$\sigma_r^A = \sigma_r^{L1} - \sigma_r^{U2} + \sigma_r^{S1}, \quad \sigma_\theta^A = \sigma_\theta^{L1} - \sigma_\theta^{U2} + \sigma_\theta^{S1} \quad (19)$$

(3) Residual stress of the elastic zone in the inner cylinder ($\rho_L < r < b$)

$$\sigma_r^A = \sigma_r^{L2} - \sigma_r^{U2} + \sigma_r^{S1}, \quad \sigma_\theta^A = \sigma_\theta^{L2} - \sigma_\theta^{U2} + \sigma_\theta^{S1} \quad (20)$$

(4) Residual stress of the elastic zone in the outer cylinder ($b < r < c$)

$$\sigma_r^A = \sigma_r^{L2} - \sigma_r^{U2} + \sigma_r^{S2}, \quad \sigma_\theta^A = \sigma_\theta^{L2} - \sigma_\theta^{U2} + \sigma_\theta^{S2} \quad (21)$$

When the plastic zone is in the outer cylinder

($b < \rho_L < c$), residual stress is expressed by Eqs. (22–25).

(5) Residual stress of the unloading stress zone ($a < r < \rho_U$)

$$\sigma_r^A = \sigma_r^{L1} - \sigma_r^{U1} + \sigma_r^{S1}, \quad \sigma_\theta^A = \sigma_\theta^{L1} - \sigma_\theta^{U1} + \sigma_\theta^{S1} \quad (22)$$

(6) Residual stress of the loading stress zone ($\rho_U < r < b$)

$$\sigma_r^A = \sigma_r^{L1} - \sigma_r^{U2} + \sigma_r^{S1}, \quad \sigma_\theta^A = \sigma_\theta^{L1} - \sigma_\theta^{U2} + \sigma_\theta^{S1} \quad (23)$$

(7) Residual stress of the loading stress zone in the inner cylinder ($b < r < \rho_L$)

$$\sigma_r^A = \sigma_r^{L1} - \sigma_r^{U2} + \sigma_r^{S2}, \quad \sigma_\theta^A = \sigma_\theta^{L1} - \sigma_\theta^{U2} + \sigma_\theta^{S2} \quad (24)$$

(8) Residual stress of the elastic zone in the outer

cylinder ($\rho_L < r < c$)

$$\sigma_r^A = \sigma_r^{L2} - \sigma_r^{U2} + \sigma_r^{S2}, \quad \sigma_\theta^A = \sigma_\theta^{L2} - \sigma_\theta^{U2} + \sigma_\theta^{S2} \quad (25)$$

3. Results and discussion

The tangential residual stress of an autofrettaged compound cylinder with various overstrain levels is shown in Fig. 9. The residual stress of an autofrettaged compound cylinder with 0.1 mm shrink fit tolerance was predicted.

From the study, it is found that the residual stress distribution of the strain-hardening model is similar to that of the elastic-perfectly plastic model, except in the compressive residual stress near the inner radius. This is because the compressive residual stresses near the inner radius decreased with the overstrain level. The compressive residual stress of the strain-hardening model is smaller than that of the elastic-perfectly plastic model because of the Bauschinger

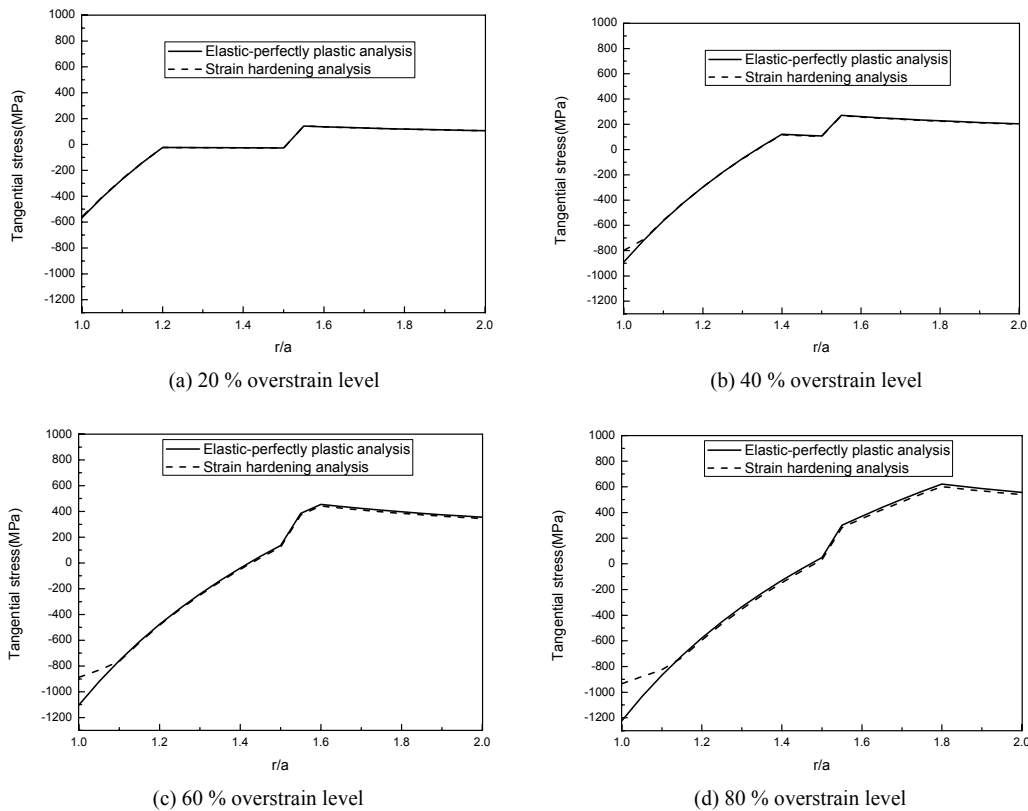


Fig. 9. Residual stress distribution of an autofrettaged compound cylinder with 0.1 mm shrink fit tolerance under various overstrain levels.

effect. That of the strain hardening model decreased by up to 80% overstrain level. The unloading stress zone increased, and reverse yielding occurred.

The differences in compressive residual stress between the two models increased with the overstrain level for the autofrettaged single cylinder. The rapid increase in tangential stress at the middle range was induced by shrink fit interaction. The shrink fit tolerance caused a compressive residual stress in the inner cylinder and a tensile residual stress in the outer cylinder. The shrink fit process is a very efficient way to increase compressive residual stress. If the tensile and compressive residual stresses will be increased at the same time, too much tolerance will be harmful to the autofrettaged cylinder.

4. Conclusions

In this study, the result of the residual stress analysis for a compound cylinder under various overstrain levels is presented. The major conclusions are as follows:

- (1) The compressive residual stress of the strain-hardening model is smaller than that of the elastic-perfectly plastic model because of the Bauschinger effect.
- (2) The compressive residual stress of the strain hardening model decreased by up to 80% overstrain level. The unloading stress zone increased, and reverse yielding occurred.
- (3) The compressive residual stress in the autofrettage experiment of a single cylinder at the inner radius has good agreement with that in strain hardening analysis. This shows that strain hardening analysis adopts a close curve-fitted stress-strain curve, which can result in better simulation of the real stress-strain relationship than the elastic-perfectly plastic model.
- (4) The shrink fit process is a very efficient way to extend compressive residual stress.

Acknowledgments

This work was supported by the Defense Acquisition Program Administration and the Agency for Defense Development of Korea under contract UD060011AD.

References

- [1] J. A. Kapp, B. Brown, E. J. LaBombard and H. A. Lorenz, On the Design of High Durability High Pressure Vessels, *Proc. ASME PVP Conference*, 371 (1998) 85-91.
- [2] R. P. Milligan, W. H. Hoo and T. E. Davidson, The Bauschinger Effect in a High-Strength Steel, *J. of Basic Eng.*, 88 (2) (1966) 480-488.
- [3] D. P. Kendall, The Bauschinger Effect in Autofrettaged Tubes-A Comparison of Models Including the ASME Code, *Proc. ASME PVP Conference*, Discussion of paper by A. P. Parker, and J. H Underwood, (1998).
- [4] R. Hill, *The Mathematical Theory of Plasticity*, Oxford University Press, (1950).
- [5] A. Stacey and G. A. Webster, Determination of Residual Stress Distributions in Autofrettaged Tubing, *International Journal of Pressure Vessels and Piping*, 33 (1998) 205-220.
- [6] X. P. Huang and W. Cui, Autofrettage Analysis of Thick-walled Cylinder Based on Tensile-compressive Curve of Material, *Key Engineering Materials*, 274-276 (2004) 1035-1040
- [7] X. P. Huang, A General Autofrettage Model of a Thick-Walled Cylinder Based on Tensile-Compressive Stress-Strain Curve of a Material", *Journal of Strain Analysis*, 40 (6) (2005) 599-607.
- [8] J. H. Park, Y. S. Lee, J. H. Kim, K. U. Cha and S. K. Hong, An Elasto-Plastic Analysis of Autofrettaged Compound Cylinders, *Proceeding of Autumn KSME Conference*, (2006) 37-42.
- [9] J. H. Park, Y. S. Lee, J. H. Kim, K. U. Cha and S. K. Hong, Machining Effect of the Autofrettaged Compound Cylinder under Varying Overstrain Level, *Journal of Material Processing Technology*, 201 (1-3) (2008) 491-496.
- [10] J. H. Park, Y. S. Lee, J. H. Kim, K. U. Cha and S. K. Hong, Machining Analysis of the Autofrettaged Compound Cylinder, *Trans. of KSME(A)*, 31 (7) (2007) 800-807.
- [11] E. Y. Lee, Y. S. Lee, Q. M. Yang, J. H. Kim, K. U. Cha and S. K. Hong, A Study on the Fatigue Life of Autofrettaged Compound Cylinder, *Trans. of KSME(A)*, 33 (4) (2009) 296-309.
- [12] F. B. Seely and J. O. Simth, *Advanced Mechanics of Materials*(Second Edition), John Wiley & Sons, (1952).
- [13] A. C. Ugural and S. K. Fenster, *Advanced Strength and Elasticity*(Third Edition), Prentice Hall, N.Y., (1995).



Eun-Yup Lee received a B.S. degree in Mechanical Design Engineering from Chungnam National University, Korea in 2007. He received master degree in Mechanical Design Engineering from Chungnam National University, Korea in 2009. He is currently researcher of LG Display company, Korea.



Qiu-Ming Yang received a B.S. degree in Mechanical Design Engineering from Dalian Polytechnic University, China in 2007. She received master degree in Mechanical Design Engineering from Chungnam National University, Korea in 2009.



Young-Shin Lee received a B.S. degree in Mechanical Engineering from Yonsei University, Korea in 1972. He received master and Ph.D. degree in Mechanical Engineering from Yonsei University, Korea in 1974 and 1980 respectively. He is currently professor and Dean of Industry Graduate School and Director of BK21 Mechatronics Group at Chungnam National University, Korea. Prof. Lee's research interests are in area of impact mechanics, optimal design, biomechanical analysis and shell structure analysis.



Jae-Hoon Kim received a B.S. degree in Precision Mechanical Engineering from Chungnam National University, Korea in 1980. He received master and Ph.D. degree in Mechanical Engineering from Chungnam National University, Korea in 1982 and 1989 respectively. He is currently professor at Chungnam National University, Korea. Prof. Kim's research interests are in area of fracture mechanics, fatigue behaviors, composite materials.